Indian Institute of Technology, Roorkee

The International Conference on Future Cities-2019

December 11-13, 2019

Indoor daylight illuminance: a comparison between experimentally determined varying CIE sky-type and a predefined CIE sky model

Naga Venkata Sai Kumar Manapragada[1] , Marshal Maskarenj[2,3]

[1]Integrative Design Solutions Pvt Ltd, Dwarka, New Delhi, India 110078

[2]Department of Energy Science and Engineering, Indian Institute of Technology Bombay, Mumbai 400076

[3]Building Energy Performance program, Faculty of Technology, CEPT University, Ahmedabad 380009

Abstract

The output accuracy of the building performance simulation tools depends on the employed models. Most daylighting simulation tools evaluate the daylight performance in built-environment through illuminance based metrics, and refer the Perez all weather model or the CIE model. Sky-luminance distribution of the ambient sky impacts the indoor daylight distribution dynamically, based on sun-position and other outdoor and indoor scattering parameters. The approach of employing the generic sky-models throughout the year could result in lower accuracy prediction of indoor illuminance distribution. This study was conducted to identify the improvement in prediction accuracy for indoor illuminance distribution, by deploying measured sky-luminance distribution data, or closest sky-model as input as compared to using a pre-defined CIE sky-model for various time instances.

Measurements from a previously reported sky-scanning device are used to identify closest sky-type which is used as a key input in simulating indoor daylight distribution. The indoor illuminance distribution is simulated for a sample space through algorithm scripted in Python (PY) and also with HoneyBee module in Rhino-Grasshopper (GH). The GH approach uses Radiance engine to perform daylight simulations for the space, and spatially discretized Indoor illuminance values are derived for uniform and varying sky type scenarios using both Python and Radiance approach.

The temporal trend in illuminance levels between PY and GH outputs is similar for same sky type through various points of the day. For uniform and varying sky types, mean standard deviation in illuminance levels of 782.1 and 238.6 lux is respectively observed between PY and GH outputs. Owing to neglecting internal reflections in PY algorithm, much reduced illuminance levels are noted, as compared to GH outputs. It is inferred that identifiers for closest CIE sky-type for various time-points may improve simulation accuracy in daylight illuminance calculations.

Keywords: Daylight illuminance; Sky-luminance distribution; CIE sky model; Daylighting simulation; Radiance.

1. Introduction

Building sector is the second highest electricity consumer, according to Ministry of Statistics and Planning Implementation (MoSPI). The Energy Statistics 2018 published by MoSPI [1] reported that building sector stake is 33% in overall consumption, with 72.7% and 37.3% contribution from residential and commercial sectors, respectively. Beside thermal comfort through air conditioning, space lighting has a significant share in the energy consumption in residential and commercial buildings. A review study inferred that the end-use contribution of space-lighting in buildings varies between 21 to 37%; as compared to the variation between 1 to 16% for comfort conditioning systems[2]. Lighting systems play a major role for task oriented purposes[3] in commercial buildings, due to less availability of perimeter zones. The daylighting provision into the built-environment must incorporate energy as well as health and well-being benefits. The studies on natural lighting and human circadian rhythms[4] inferred that natural light helps maintain the biological clock, whereas artificial lighting may cause late sleep schedules and disrupt sleep.

While adding daylighting in space could help reduce artificial lighting usage, it could lead to heat gains through solar ingress. Techniques like solar shelves, static and dynamic shading systems can address solar heat gains attributed with daylighting, but designing appropriate and effective passive and active strategies requires tools to simulate typical annual conditions. The introduction of computational systems for optimally solving complex problems has enabled the research community with tools for daylight evaluation in built-environment. However, the accuracy of these tools depends on the model employed for evaluation. Daylight simulation packages employ Perez all-weather sky model or the CIE standard model for annual calculations, and it is reported that models underestimate the prediction of indoor daylight illuminance as compared to measured data owing to smoothening of temporal sky-conditions[5]. Since the outdoor sky-conditions vary dynamically, it is important to incorporate these changes into the simulation models. This study aims to evaluate the accuracy of the daylighting results by comparing outputs with uniform/generic sky-type and experimentally assessed varying sky-type used as key-input.

2. Research Methodology

Indoor daylight illuminance distribution at discrete points depends on the luminance of discrete sky patches 'as seen' at those points, which is affected by the view angle of building fenestrations[6]. Other than sky-component of daylight, attributes like reflections from surrounding structures (externally reflected component) and reflections from indoor surfaces (internally reflected component) contribute to the net daylight distribution indoors. This study took a case of a sample apartment as shown in Fig. 1(a) and 1(b) for evaluating the variance in daylighting simulation output for generic and varying sky types. Available tools for daylight simulations use CIE sky-models for point in time calculations, and Perez all-weather sky model[7] for annual simulations as default. This paper discusses simulations performed for point-in-time calculations, using temporally-discretized CIE skypes as the test scenario, while keeping a case with generic sky-model for all time-points as the alternative scenario. To perform indoor daylight illuminance simulations using temporally-varying sky-models, the closest CIE sky-model for various time-points was needed, and identification of closest sky-model for a point-in-time is described as follows.

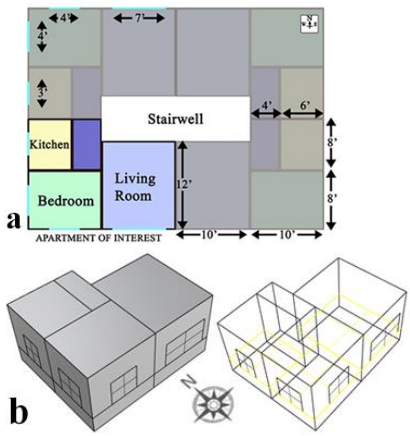

Fig.1. (a) Plan of the apartment layout (b) 3D model of the apartment layout

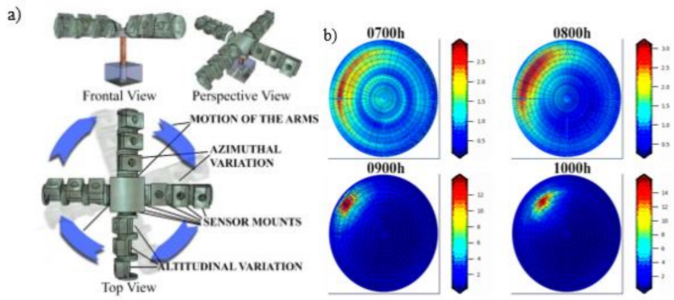

Fig. 2.(a) Sky scanning device with Fresnel-like design (b) Sky maps for 30-1-2018 for 1-hour interval.

2.1. Identification of closest CIE sky-type

Maskarenj, Banerjee, et al. [8] developed a Sky scanning device with Fresnel-like design to measure and record the sky luminance of each patch over extended periods. The device demonstrated in Fig. 2(a) measures sky-luminance at various altitude-by-azimuthal positions of the sky-hemisphere with 5-minute intervals, and may be used for generating hourly sky luminance map (Fig. 2b) for the annual daylight-hours for a selected location. This study employs datasets measured and analyzed for 30-January-2018 at Mumbai, India with the reported closest CIE-sky types as hourly-varying key-input for indoor-daylight analysis. The CIE sky-model is capable of generating 15 different sky types – 5 each for overcast, intermediate and clear sky conditions. The gradient and scattering components define the sky-turbidity combination levels which intact suffice to classify sky-type as clear, intermediate or overcast. The coefficients 'a' and 'b' in Table 1 represent the gradation component of sky from Zenith to Horizon, whereas coefficients 'c', 'd' and 'e' represent the scattering component of the model. The luminance ratio of any sky patch with respect to zenith luminance is dependent on the gradation and scattering functions.

As mentioned previously, the sky-luminance at any angle with respect to the zenith depends on the scattering and gradation behaviors[9]. The luminance gradation function 'φ' for a sky-patch at a defined Zenith angle 'Z' (with respect to zenith) is described in Eq.1, and Eq.2 describes the gradation behavior at Zenith (Z=0°). The scattering function 'f' also affects the luminance distribution behavior, and the scattering function for a sky-patch at an angle 'χ' with respect to sun is given by Eq.3; since the sun-angle with Zenith is the same as zenith angle of sun (Z_s), the scattering function for Z_s is presented in Eq.4.

$$\varphi(Z) = 1 + a.exp(b/cosZ) \quad (1) \qquad \varphi(0°) = 1 + a.exp(b) \quad (2)$$

$$f(\chi) = 1 + c.(exp(d.\chi) - exp(d.\pi/2)) + e.cos2\chi \quad (3) \qquad f(Zs) = 1 + c.(exp(d.Zs) - exp(d.\pi 2)) + e.cos2Zs \quad (4)$$

Coefficients *a*, *b*, *c*, *d* and *e* depend on the sky-type, and the coeffiients for 15 most-occurent CIE sky-types are previously reported. Maskarenj, Chawla, et al. [10] have presented a measurement-based method for identifying the most occurring sky-types for a location based on frequency of occurrence, and have used the root mean square deviation (RMSD) approach to identify closest sky-type for various time-points. The approach evaluates sun-position and normalized luminance ratios for 265 sky-positions, derived from luminance data measured between 0700 hours to 1800 hours for various test-days, and the deduced closest-sky types are reported for Mumbai, India. Selection is done based on minimum RMSD for zenith-normalized luminance ration for all sky-patches between measured datasets and modeled datasets for all 15 CIE sky-types. These reported closest sky-type data was used as a key-input in this study for predicting indoor daylight illuminance distribution. For a test day, the closest CIE sky at various time-points is presented in Table 1.

Table 1. CIE and Radiance sky-types at various hours of the day on 30 Jan 2018 (Mumbai)

Time	CIE Sky	CIE Definition	GH Sky	GH Definition
07:00	4	Overcast, moderately graded, slight brightening near Sun	4	Cloudy sky,
08:00	6	Partly Cloudy sky, slight brightening near Sun	3	Intermediate without sun
09:00	8	Partly Cloudy sky, No gradation, distinct solar corona	2	Intermediate with sun
10:00	8		2	
11:00	8		2	
12:00	13	CIE Standard Clear Sky, polluted atmosphere	0	Sunny with sun
13:00	13		0	
14:00	13		0	
15:00	8	Partly Cloudy sky, No gradation, distinct solar corona	2	Intermediate with sun
16:00	8		2	
17:00	8		2	
18:00	6	Partly Cloudy sky, slight brightening near Sun	3	Intermediate without sun,

2.2. Indoor Daylight illuminance distribution prediction

An algorithm is scripted in Python to calculate net sky-illuminance at any point indoors, as described in Eq. 5. The window-based net-sky component is evaluated for any point (I_{net}): here, the internally and externally reflected components of daylight are not considered by the Python-based approach (PY) for simplicity of calculations.

$$I_{net} = \sum_{i=0}^{N_\alpha} \sum_{j=0}^{N_\gamma} L_{\gamma_j \alpha_i} * sin(\gamma_j) * cos(\gamma_j) * cos(\alpha_{w_i}) * \Delta_\gamma \Delta_\alpha \qquad (5)$$

Here, α corresponds to the azimuth angle, γ corresponds to altitude angle, 'i' and 'j' are step-angles limited from minimum (0) to maximum (N) segments of the window, and the summation is done over unit incremental values of 'Δγ' and 'Δα' at 1° each. The illuminance distribution is the generated dataset of the individual illuminance data at various positions across the room. The calculations in this paper are performed for a sample apartment block, presented in Fig. 1(a). The simplified design is shown: the window-sill is about 2.6' (0.8m) above floor level, window height is about 3.9' (1.2m) and the ceiling height is 9.8' (3m) above floor.

3. Analysis

The PY algorithm calculated illuminance distribution at various discrete points in the three rooms with window access: Living Room with south-facing window, Kitchen with west-facing window and bedroom with two windows facing south and west. Calculations are performed at various points in time using measured dataset and dataset from CIE overcast sky-model, and collated indoor illuminance maps are demonstrated in Fig. 3(a) for three rooms, along with sky-luminance maps of the ambient sky at that time-point. The scale for indoor illuminance maps is the same in both cases.

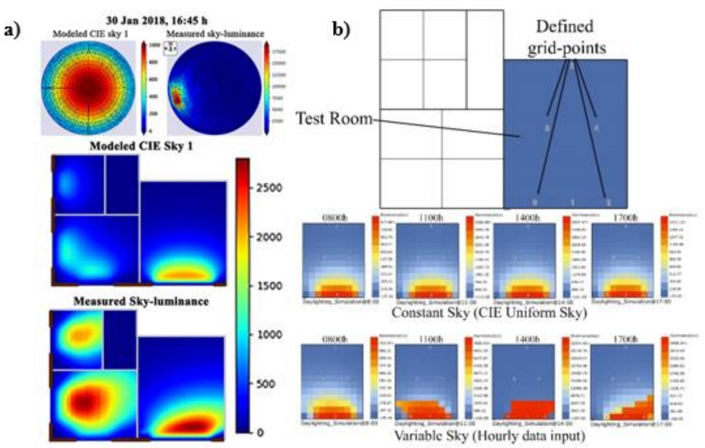

Fig.3. (a) Measured and modelled (CIE overcast) sky-luminance maps and corresponding indoor illuminance maps calculated via original Python script for sample test cases (b) Indoor illuminance maps generated for various time-points for constant and variable sky-types.

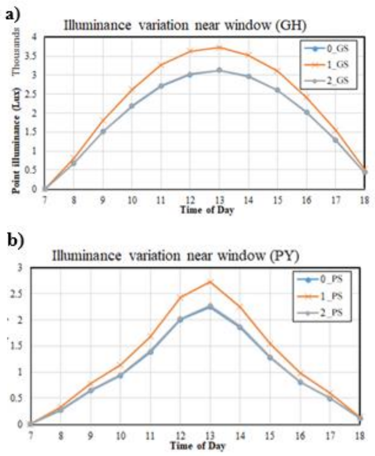

Fig. 4. Temporal variation in Indoor illuminance for constant sky-type: a) GH, b) PY model

In GH approach, for constant sky-type (Uniform sky), the input to *"genStandardCIESky"* in Group 2 was set at 5, and for varying sky, the input was varied for each hour as presented in Table 1. The grid-points marked 1 to 6 in the living room are presented in Fig. 3(b), along with illuminance maps for various time-points for constant and variable sky-types.

4. Results

Illuminance data is extracted in GH for the six defined locations for Variable sky and Constant sky at different points in time, and similar datasets are generated from the PY approach. As connotation, GS refers to Grasshopper calculations and PS refers to Python calculations to Sky 1. Fig 4 shows the temporal variation in indoor illuminance for points 0, 1, and 2 located near the window for all time points, and Fig 3b represents daylight illuminance distribution for all spatially discretised positions for few time-points spread across 3-hour interval. The much-higher illuminance values calculated for varying sky models (GH) are due to the solar ingress at the points near the window, as seen in Fig 4(b). Mean standard deviation of 782.1 lux and 238.6 between GH and PY outputs for the constant and varying sky types is due non-inclusion of internal reflection in PY algorithm.

5. Discussions and future scope

Fig 5 demonstrates the variation of daylight distribution pattern between constant and variable sky types. By incorporating actual measurements in place of CIE or other sky-models, the accuracy of indoor illuminance assessment may be improved, and the output could be made compatible with other modules for building performance simulation. Through Rhino-Grasshopper, components based on LadyBug and HoneyBee modules can be scripted that can perform annual daylighting simulation with varying sky type. The same component can also suffice the architects in developing strategies to evenly distribute daylighting and provide glare control.

6. Conclusion

This work uses measurements from original sky-luminance measurement device and uses a Python algorithm for generating illuminance distribution datasets for the interiors of built space. To compare this approach in a validated tool, the indoor illuminance calculations are done in Grasshopper plugin of Rhino, using Ladybug and HoneyBee tools. To address the simulation tool constraints, measured datasets are reduced to closest CIE sky-models, and are further converted to corresponding models allowed in Grasshopper/Radiance. The indoor positions receiving high solar ingress from circumsolar region exhibit good match, but positions exposed to low-luminance sky-patches (non-circumsolar regions) show deviation in GH and PY data. This may be attributed to 'smoothening' of model-generated data at various sky-positions -- as compared to actual sky-luminance data; and the lack internally reflected component of daylight in PY approach. The approach still yields better results as compared to applying generic models across all time-points.

Bibliography

1. Ranganadham M. *Energy Statistics 2018*. New Delhi; 2018. http://mospi.nic.in/sites/default/files/publication_reports/Energy_Statistics_2018.pdf.
2. Chunekar A, Varshney S, Shantanu D. *Residential Electricity Consumption in India*. Pune; 2016. http://www.prayaspune.org/peg/publications/item/331-residential-electricity-consumption-in-india-what-do-we-know.html.
3. Osterhaus WKE. Office lighting: a review of 80 years of standards and recommendations. In: *Proceedings of the 1993 IEEE Industry Applications Society Annual Meeting*. ; 1993:2365–2374.
4. Wright KP, McHill AW, Birks BR, Griffin BR, Rusterholz T, Chinoy ED. Entrainment of the human circadian clock to the natural light-dark cycle. *Curr Biol*. 2013. doi:10.1016/j.cub.2013.06.039
5. Inanici M, Hashemloo A. An investigation of the daylighting simulation techniques and sky modeling practices for occupant centric evaluations. *Build Environ*. 2017. doi:10.1016/j.buildenv.2016.09.022
6. Kittler R, Darula S. Scattered sunlight determining sky luminance patterns. *Renew Sustain Energy Rev*. 2016. doi:10.1016/j.rser.2016.05.012
7. Perez R, Seals R, Michalsky J. All-weather model for sky luminance distribution-Preliminary configuration and validation. *Sol Energy*. 1993. doi:10.1016/0038-092X(93)90017-I
8. Maskarenj M, Banerjee R, Ghosh PC. Design and development of a low-cost angular sky luminance measurement system. *Build Environ*. 2018. doi:10.1016/j.buildenv.2018.06.001
9. Darula S, Kittler R. CIE General sky standard defining luminance distributions. In: *ESim 2002: The Canadian Conference on Building Energy Simulation*. ; 2002.
10. Maskarenj M, Chawla G, Banerjee R, Ghosh PC. Evaluation of dynamic sky-type using novel angular sky luminance measurement system. *Build Environ*. 2018. doi:10.1016/j.buildenv.2018.09.051